Research in Astronomy and Astrophysics, 24:125013 (13pp), 2024 December https://doi.org/10.1088/1674-4527/ad8f9c

BSN: The First Photometric Analysis of Contact Binary Systems V1961 Cyg and V0890 Lyr

Sabrina Baudart[1] and Atila Poro[2]
[1] Double Stars Committee, Société Astronomique de France, Paris, France; sabrina.baudart@gmail.com
[2] LUX, Observatoire de Paris, CNRS, PSL, 61 Avenue de l'Observatoire, 75014 Paris, France
Received 2024 September 10; revised 2024 October 18; accepted 2024 November 5; published 2024 December 4

Abstract

We presented the first photometric analysis of the V1961 Cyg and V0890 Lyr binary systems. We observed and analyzed these systems at an observatory in France as part of the Binary Systems of South and North (BSN) Project. We extracted and collected the times of minima from the observations and literature and presented a new ephemeris for each system. Due to the few observations about these systems over the years, both O–C diagrams were fitted linearly. The PHysics Of Eclipsing BinariEs (PHOEBE) Python code and the Markov Chain Monte Carlo (MCMC) method were used for light curve solutions. The light curve solution required a cold starspot on the hotter component in the V1961 Cyg binary system. We compared and have close agreements between our mass ratios' results from the light curve analysis processes and a new method based on the light curve derivative. We estimated the absolute parameters using an empirical relationship between the semimajor axis and orbital period for contact binary systems. The results show V1961 Cyg and V0890 Lyr are W-type contact binary systems. We displayed stars and systems' positions in the *M–L*, *M–R*, and $\log M_{\rm tot} - \log J_0$ diagrams. We also presented a new relationship between mass ratio and luminosity ratio.

Key words: (stars:) binaries: eclipsing – methods: observational – stars: individual (V1961 Cyg, V0890 Lyr)

1. Introduction

Two late-type stars in W Ursae Majoris (W UMa) eclipsing contact binary systems have short orbital periods. The two components overfill their critical Roche lobes in these systems and share a common envelope (Kopal 1959). The effective temperature difference between the component stars in contact binary systems is low, and they additionally have a close or equal depth of minima (Kuiper 1941; Yakut & Eggleton 2005).

W UMa contact binaries are generally classified into two categories: A-subtype and W-subtype (Binnendijk 1970). The subtype of a system cannot be recognized only from its light curve shape, and it is required to estimate its absolute parameters, including the mass of the stars (Guo et al. 2022).

The stars of contact systems are transferring mass to each other (Lucy & Wilson 1979); in this process, their orbital periods can be changed. The orbital period of contact systems plays a role in relations with absolute parameters, and they are effective in the evolutionary process of these systems (Latković et al. 2021; Loukaidou et al. 2022; Poro et al. 2024b, 2024c). Several studies have been conducted on the upper and lower cut-offs of these systems' orbital periods (Zhang & Qian 2020).

Asymmetric light curves acquired from contact and near-contact binaries are commonly observed over time, especially at phases 0.25 and 0.75. This phenomenon is generally referred to as the O'Connell effect (O'Connell 1951), which is crucial for studying a star's magnetic activity. This asymmetry in the light curves is solved with one or more starspot(s) and is challenging in the modeling.

In this work, we investigated V1961 Cyg (2MASS J21243169+3957197) and V0890 Lyr (2MASS J19184581 +3708166) which are binary star systems classified as EW type in variable star catalogs and databases such as ASAS-SN,[3] GCVS,[4] ZTF[5], VSX.[6]

The variability of V1961 Cyg (2MASS J21243169 +3957197) was discovered by Kulagin & Shugarov (1989). Based on Gaia Data Release 3 (DR3), V1961 Cyg has coordinates of R.A.: 321.°1320 and decl.: 39.°9554 in the Cygnus constellation. This system ranges from 13.88 to 14.6 mag in the *V* filter, according to the VSX database. The orbital period of V1961 Cyg was reported to be 0.286008 days in the Kulagin & Shugarov (1989) study and 0.2860135 days in the ASAS-SN catalog of variable stars.

In the survey of the Two Micron All Sky Survey (2MASS) and the Northern Sky Variability Survey (NSVS) data, V0890 Lyr was found (Gettel et al. 2006). This system is located in the constellation Lyra with coordinates of R.A.: 289.°6909 and decl.: 37.°1379, according to the Gaia DR3 database. The VSX

[3] The All Sky Automated Survey, https://asas-sn.osu.edu/variables.
[4] General Catalogue of Variable Stars.
[5] The Zwicky Transient Facility.
[6] International Variable Star Index, https://www.aavso.org/vsx/.

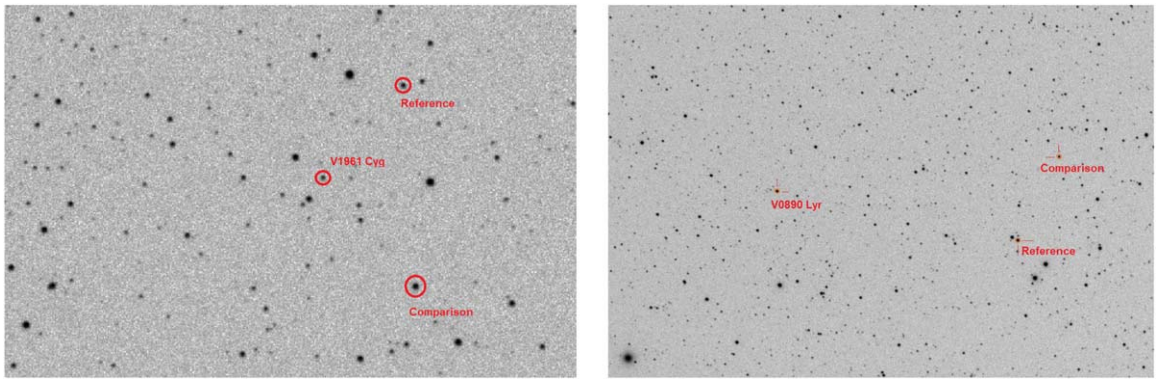

Figure 1. The left side is the field-of-view of the V1961 Cyg binary system, and the right side is for V0890 Lyr, together with the comparison and check stars used in the observations.

database reported a magnitude range of 11.38–11.71 mag in the *V* filter and an orbital period of 0.3884152 days for V0890 Lyr.

We aim to investigate two contact binary systems that have not been previously studied. Different systems have their own characteristics, and their analysis can lead to a better understanding of them. Also, investigating new contact binary systems might result in a larger sample of the studied targets, which could be used to study future empirical parameters. This paper's structure is as follows: Section 2 describes the observational data and methods used for data reduction. Section 3 presents the new ephemeris of each contact binary system. In Section 4, we present the solution of the light curve analysis, while Section 5 provides the estimated absolute parameters of each target system. Finally, Section 6 gives our discussion and conclusion.

2. Observation and Data Reduction

We observed V1961 Cyg and V0890 Lyr at a private observatory located in Toulon, France (longitude 05° 54" 35" E, latitude 43° 8' 59" N, altitude 68 m above sea level). The photometric observations were made using the standard *V* filter for both target systems. We employed an apochromatic refractor telescope with a 102 mm aperture and a ZWO ASI 1600MM CCD to observe the V1961 Cyg and V0890 Lyr binary systems. The binning of the images was 1 × 1, and the average temperature during the observations was −15°C.

V1961 Cyg was observed for three nights on July 2nd, 9th, and 13th, 2023, accumulating 499 images with 110 s of exposure time. We used Gaia DR2 1965471833170939904, whose magnitude is $V = 12.795(28)^{\mathrm{mag.}}$ and coordinates are R.A.: $21^{\mathrm{h}}24^{\mathrm{m}}21\overset{\mathrm{s}}{.}976$, decl.: +39°59′36.″83, as a comparison star. Gaia DR2 1965424588530688256 was chosen as a check star with a magnitude of $V = 13.621(34)^{\mathrm{mag}}$ and coordinates R.A.: $21^{\mathrm{h}}24^{\mathrm{m}}22\overset{\mathrm{s}}{.}725$, decl.: +39°55′27.″37 (Figure 1, left). Our observations' average signal-to-noise ratio (SNR) is 15.49 decibels (dB), which indicates a 0.03 mag uncertainty for V1961 Cyg.

V0890 Lyr was observed for two nights on August 19th and 20th, 2023. These observations resulted in 484 images with an exposure time of 80 s. Gaia DR2 2051151521582207232 (R.A.: $19^{\mathrm{h}}17^{\mathrm{m}}06\overset{\mathrm{s}}{.}764$, decl.: +37° 06′03.″74, $V = 12.672(140)^{\mathrm{mag}}$) was used as a check star, and Gaia DR2 2051169835322822912 (R.A.: $19^{\mathrm{h}}17^{\mathrm{m}}21\overset{\mathrm{s}}{.}475$, decl.: +37°11′52.″05, $V = 11.439(119)^{\mathrm{mag}}$) as a comparison star (Figure 1, right). Our data analysis indicates that the average SNR is 24.56 dB, which means an uncertainty of 0.004 mag for V0890 Lyr.

The field-of-view of the target systems with comparison and check stars is shown in Figure 1.

We obtained each light curve's apparent magnitude of maximum brightness based on our observations. This resulted in $V_{\mathrm{max}} = 13.83(37)$ magnitude for V1961 Cyg and $V_{\mathrm{max}} = 11.627(90)^{\mathrm{mag}}$ for V0890 Lyr.

The data reduction process for both binary systems involved standard calibration techniques, including the correction for bias using offset frames, subtraction of dark frames to eliminate thermal noise, and division by flat-field frames to correct for uneven illumination. These standard processes were executed using the 1.2.0 version of the Siril software.[7]

3. New Ephemeris

Data derived from our ground-based observations were used to extract primary and secondary times of minima. We utilize a Python program to fit a Gaussian distribution and extract minima from ground-based data (Table 1). We used the online tool[8] to convert the times of minima gathered in the literature, which were Heliocentric Julian Day (HJD) to Barycentric Julian Date and Barycentric Dynamical Time (BJD_{TDB}). The times of minima are listed in Table 1.

[7] https://siril.org/fr/download/2023-09-15-siril-1.2.0/
[8] https://astroutils.astronomy.osu.edu/time/hjd2bjd.html

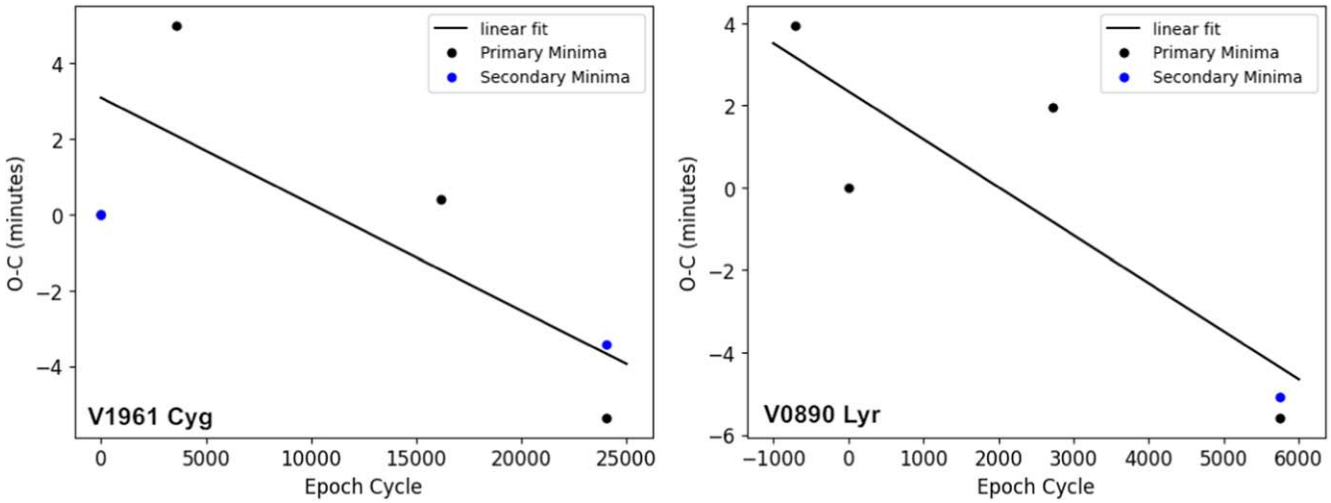

Figure 2. The left panel displays the O–C diagram for V1961 Cyg, while the right panel shows the O-C diagram for V0890 Lyr.

Table 1
Available CCD Times of Minima from this Study and Literature for V1961 Cyg and V0890 Lyr Binary Systems

System	Min.(BJD_{TDB})	Error	Epoch	O–C	References
V1961 Cyg	2457891.08346	...	16,194	0.0003	ASAS-SN
	2454291.60675	...	3609	0.0035	VSX
	2453259.38056	0.00240	0	0.0000	Hubscher et al. (2005)
	2453259.52356	0.00280	0.5	0.0000	Hubscher et al. (2005)
	2460135.57174	0.08059	24041.5	−0.0024	This study
	2460139.43157	0.06740	24,055	−0.0037	This study
V0890 Lyr	2457944.979491	...	0	0.00000	VSX
	2457670.761095	...	−706	0.00274	ASAS-SN
	2459003.412275	...	2725	0.00136	Pagel (2022)
	2460176.420936	0.000241	5745	−0.00388	This study
	2460177.392328	0.000442	5747.5	−0.00352	This study

A reference ephemeris was used to calculate the epoch and O–C values of each system. We chose $t_0(BJD_{TDB}) = 2453259.38056 \pm 0.00240$ from the Hubscher et al. (2005) study and $P_0 = 0.2860135$ days from the ASAS-SN catalog for the V1961 Cyg system. V0890 Lyr's $t_0(BJD_{TDB}) = 2457944.979491$ and $P_0 = 0.3884152$ days came from the VSX database. O–C diagrams of the systems are presented in Figure 2. The O–C diagram of each system was fitted linearly based on the few observations available for these target systems.

We computed new ephemerides for these systems (Equations (1) and (2)):

$$\begin{cases} V1961\ \text{Cyg:} \\ BJD_{TDB}(\text{Min.}I) = 2453259.38270(184) + 0.28601330(13) \times E \end{cases} \quad (1)$$

$$\begin{cases} V0890\ \text{Lyr:} \\ BJD_{TDB}(\text{Min.}I) = 2457944.98112(121) + 0.3884144(4) \times E \end{cases} \quad (2)$$

where E is the number of orbital cycles after the reference mid-eclipse time.

4. Light Curve Solutions

We employed the PHysics Of Eclipsing BinariEs (PHOEBE) 2.4.9 Python code and the Markov Chain Monte Carlo (MCMC) method in this investigation (Prša et al. 2016; Conroy et al. 2020) to provide the first light curve analysis of the binary systems V1961 Cyg and V0890 Lyr. We have chosen a contact mode in the PHOEBE code based on the classification given to both systems in the catalogs and the typical shape of their light curves. The assumed gravity-darkening coefficients and

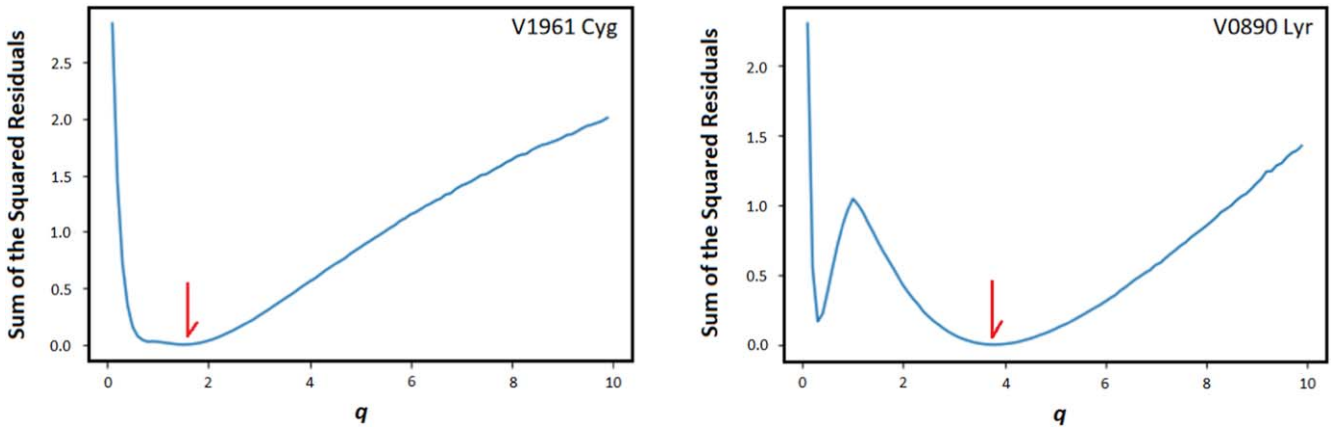

Figure 3. Sum of the squared residuals as a function of the mass ratio.

bolometric albedo in this study are respectively $g_h = g_c = 0.32$ (Lucy 1967) and $A_h = A_c = 0.5$ (Rucinski 1969). A stellar atmosphere model has been applied under the Castelli & Kurucz (2004) method, and limb-darkening coefficients were determined by using PHOEBE.

We considered the Gaia DR3[9] reported temperatures (5386 K) on the hotter component of V1961 Cyg as an initial value based on the light curve morphology. TESS reported a temperature for V1961 Cyg to be 5157 ± 224 K. For the V0890 Lyr system, we set the effective temperature provided by the TESS database (6876 K) on the hotter component. Gaia DR3 did not report the V0890 Lyr system's temperature, while Gaia Data Release 2 (DR2) indicates it as 6911 K. Then, we used the depth difference between the light curve's primary and secondary minima to determine the temperature ratio of each system.

We determined the initial value of the mass ratio using photometric data. So, we performed a q-search with a 0.1 step, ranging from 0.1 to 10. Figure 3 illustrates that each q-search curve has a clear minimum sum of squared residuals. Then, we tried to obtain a good initial theoretical fit to the observational data.

The light curve of the V1961 Cyg contact binary system shows asymmetry in the peak brightness. The difference between the maxima of the light curve for V1961 Cyg is 0.068^{mag}. This is a sign of the O'Connell effect, for which one explanation might be the existence of a starspot due to magnetic activity on the star's surface (O'Connell 1951). Accordingly, one cold starspot has been added to the hotter component of the V1961 Cyg system. This starspot position and characteristic is described in Table 2, and it is visible in the three-dimensional (3D) representation of V1961 Cyg in Figure 7.

[9] https://gea.esac.esa.int/archive/

Table 2
Photometric Light Curve Solution Results for V1961 Cyg and V0890 Lyr

Parameter	V1961 Cyg	V0890 Lyr
T_h (K)	$5415^{+(7)}_{-(7)}$	$7017^{+(12)}_{-(18)}$
T_c (K)	$5128^{+(6)}_{-(6)}$	$6779^{+(15)}_{-(14)}$
$q = M_c/M_h$	$1.519^{+(36)}_{-(26)}$	$3.778^{+(46)}_{-(27)}$
$\Omega_h = \Omega_c$	4.432(9)	7.437(12)
i°	$88.57^{+(56)}_{-(52)}$	$66.89^{+(21)}_{-(21)}$
f	$0.211^{+(5)}_{-(5)}$	$0.305^{+(9)}_{-(11)}$
$l_h/l_{\mathrm{tot}}(V)$	$0.482^{+(4)}_{-(4)}$	$0.264^{+(4)}_{-(4)}$
$l_c/l_{\mathrm{tot}}(V)$	0.518(3)	0.736(5)
$r_{(\mathrm{mean})h}$	0.362(7)	0.289(7)
$r_{(\mathrm{mean})c}$	0.434(8)	0.515(8)
Phase shift	−0.01(1)	−0.01(1)
$\mathrm{Colatitude}_{\mathrm{spot}}$(deg)	$100^{+(3)}_{-(3)}$	...
$\mathrm{Longitude}_{\mathrm{spot}}$(deg)	$284^{+(3)}_{-(2)}$	...
$\mathrm{Radius}_{\mathrm{spot}}$(deg)	$24.98^{+(65)}_{-(71)}$	...
$T_{\mathrm{spot}}/T_{\mathrm{star}}$	$0.873^{+(12)}_{-(15)}$	...
Component	Hotter	...

Then, we used PHOEBE's optimization tool to improve the theoretical fit. Finally, we applied the MCMC approach, which is based on the emcee package (Foreman-Mackey et al. 2013) in PHOEBE, to determine the values of the parameters together with their uncertainty (Hogg & Foreman-Mackey 2018). This process took into account a normal Gaussian distribution within the range of solutions for inclination (i), the mass ratio (q), fillout factor (f), effective temperatures for both components ($T_{1,2}$), and the luminosity of the primary star (l_1). Four starspot parameters were also added for the V1961 Cyg system's MCMC process. The MCMC approach was employed with 96 walkers and 1500 iterations for V1961 Cyg, and 96 walkers and 1000 iterations for V0890 Lyr.

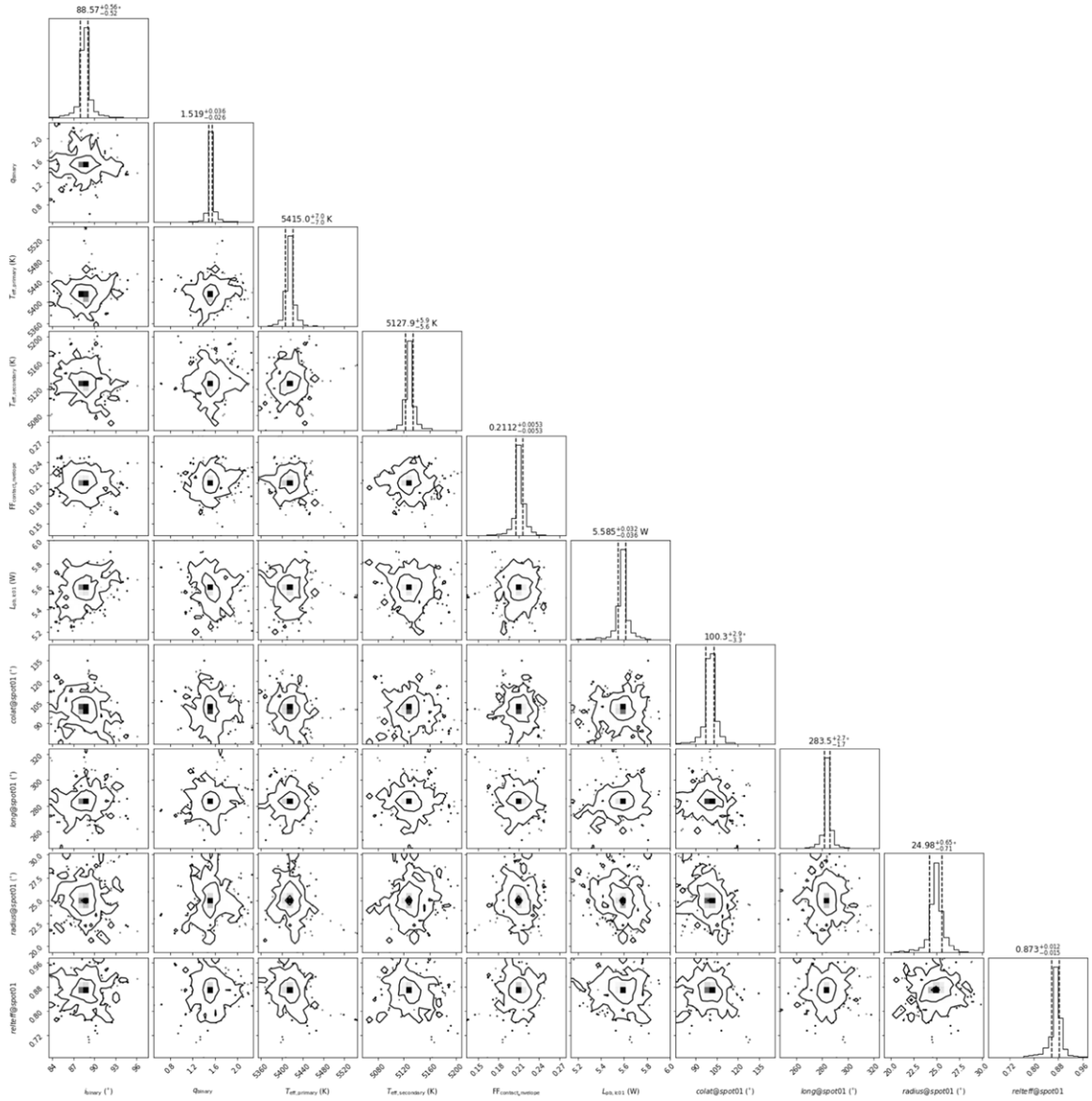

Figure 4. Determined corner plots of V1961 Cyg by the MCMC processing.

The photometric light curve solution results are listed in Table 2 and the corner plots produced by the MCMC modeling for each system are shown in Figures 4 and 5. The observational and synthetic light curves for the V1961 Cyg and V0890 Lyr systems are displayed in Figure 6.

5. Absolute Parameters

The empirical relationship between the semimajor axis (a) and orbital period (P) from the Poro et al. (2024a) study was utilized as the foundation for estimating the absolute parameters of each target system (Equation (3)).

$$a = (0.372^{+0.113}_{-0.114}) + (5.914^{+0.272}_{-0.298}) \times P. \quad (3)$$

We presented the orbital period of the systems as 0.28601330(13) days for V1961 Cyg and 0.3884144(4) days for V0890 Lyr. Using these values, we have computed $a(R_{\odot})$ from Equation (3).

Equation (4) was used to estimate the radii of stars based on the $r_{\mathrm{mean}(h,c)}$ which resulted in the light curve solutions, and the value of a.

$$R_{(h,c)} = a \times r_{\mathrm{mean}(h,c)}. \quad (4)$$

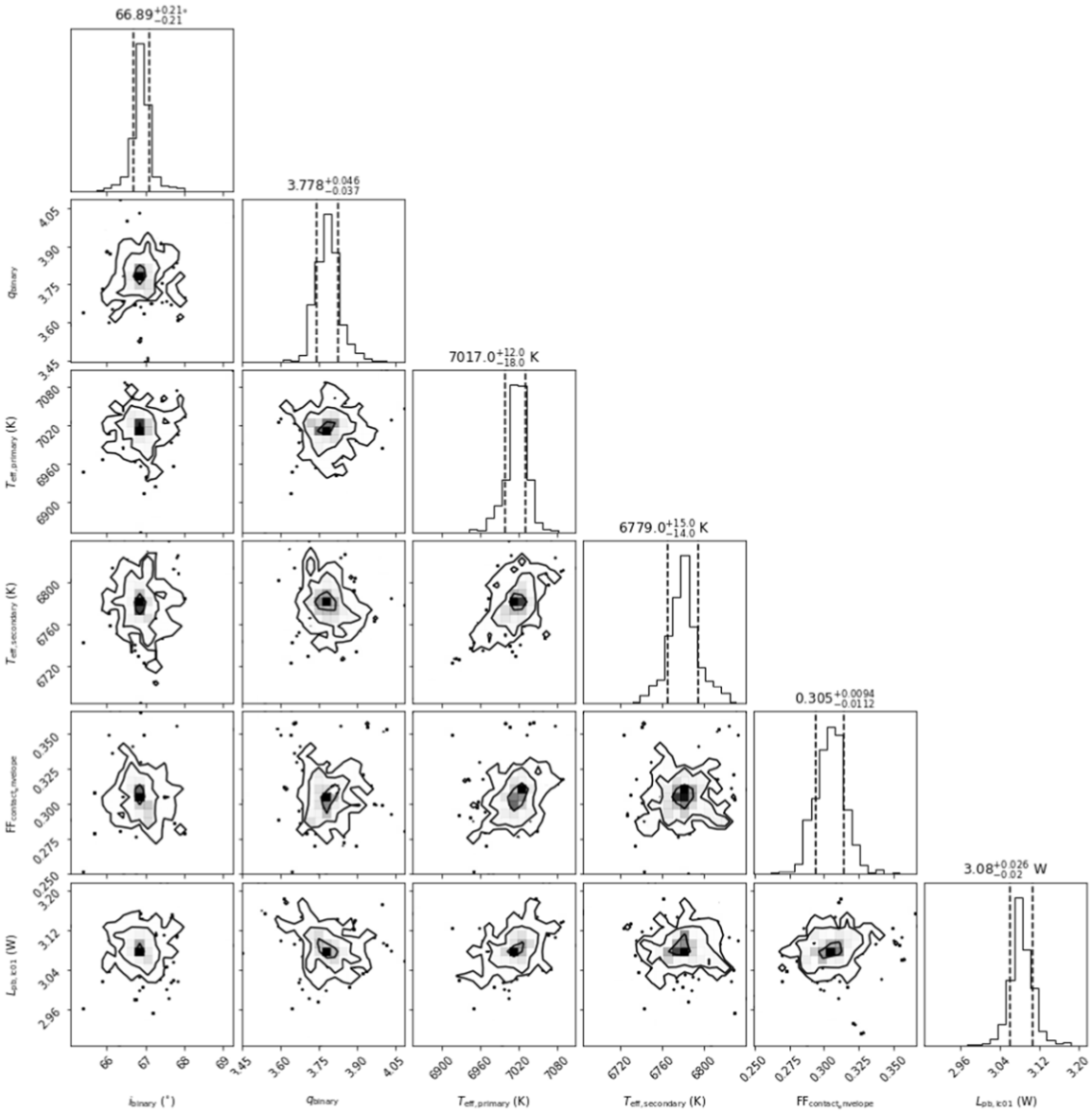

Figure 5. Determined corner plots of V0890 Lyr by the MCMC processing.

The effective temperature of each component has also been found in the light curve solutions. Considering a blackbody emission, we computed the luminosity $L_{(h,c)}(L_{\odot})$ from the radius of each component and its effective temperature (Equation (5)).

$$L_{(h,c)} = 4\pi\sigma {T_{(h,c)}}^4 {R_{(h,c)}}^2. \quad (5)$$

The mass ratio and well-known Kepler's third law were used to estimate each component's mass. The stars' mass values were computed by Equations (6) and (7).

$$M_h = \frac{4\pi^2 a^3}{GP^2(1+q)}, \quad (6)$$

$$M_c = q \times M_h. \quad (7)$$

Next, the surface gravity of each star is determined using its mass and radius by Equation (8).

$$\log(g_{(h,c)}) = \log\left(\frac{GM_{(h,c)}}{R^2_{(h,c)}}\right). \quad (8)$$

Finally, using the Pogson (1856) study, we were able to compute the absolute bolometric magnitudes ($M_{\mathrm{bol}(h,c)}$) of each component (Equation (9)). We used the solar bolometric magnitude value reported from the Torres (2010) study, which is

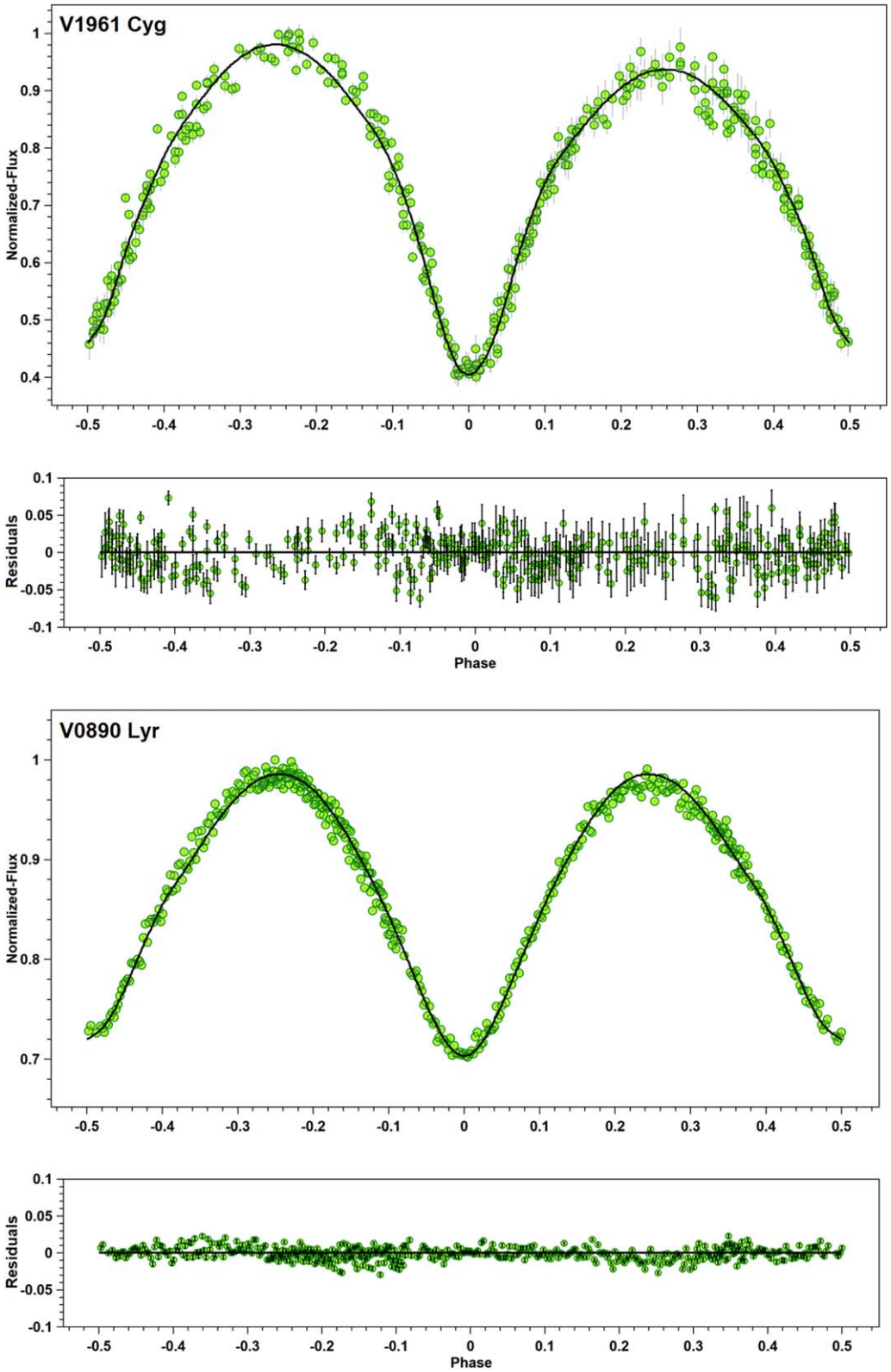

Figure 6. Light curves from observational data (green dots) and the best theoretical fit (black line) are presented for V1961 Cyg and V0890 Lyr. Residuals are displayed on the bottom panel of each light curve.

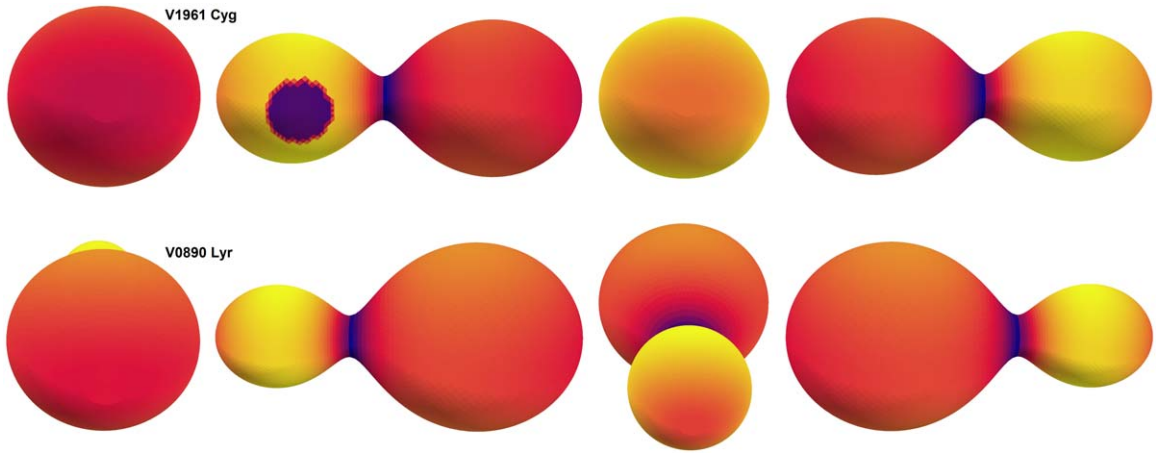

Figure 7. 3D representation of V1961 Cyg (top) and V0890 Lyr (bottom). The displayed phases are 0, 0.25, 0.5, and 0.75.

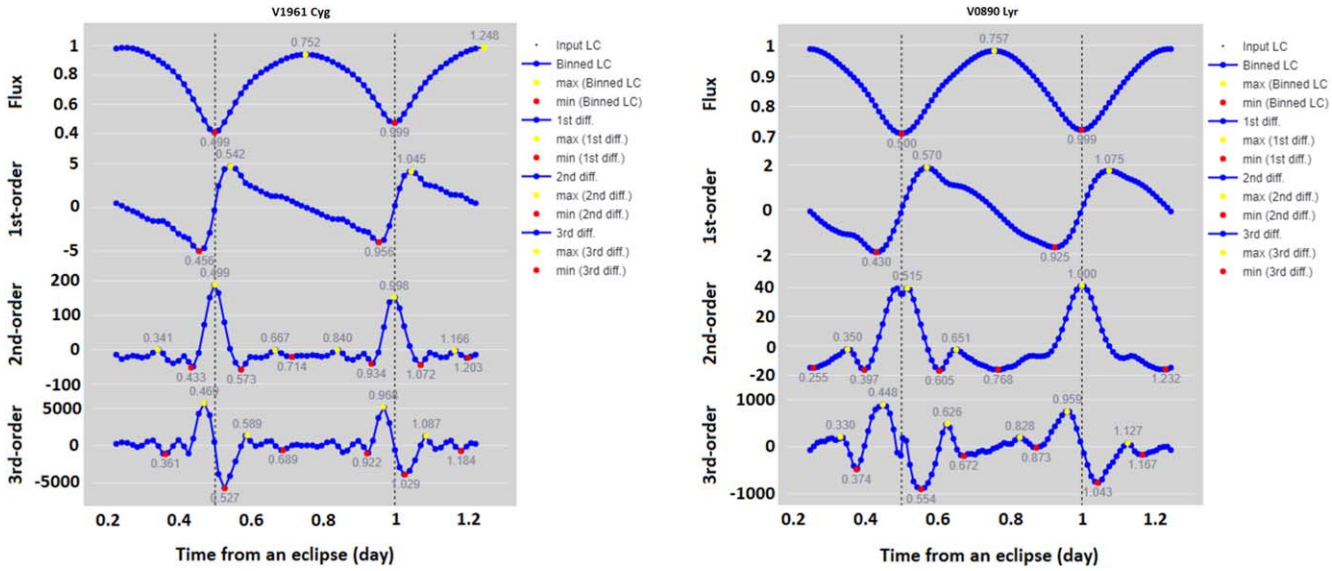

Figure 8. The light curve of V1961 Cyg (left) and V0890 Lyr (right), and first to third derivatives (top to bottom panels), respectively. The units of the panels on the vertical axis from top to bottom are W m^{-2}, 10 W m^{-2} day^{-1}, 10^2 W m^{-2} day^{-2}, and 10^4 W m^{-2} day^{-3}, respectively.

Table 3
Absolute Parameter Estimation Results

	V1961 Cyg		V0890 Lyr	
Parameter	Hotter Star	Cooler Star	Hotter Star	Cooler Star
$M(M_\odot)$	0.572(178)	0.870(294)	0.354(93)	1.338(369)
$R(R_\odot)$	0.747(86)	0.896(103)	0.771(85)	1.375(139)
$L(L_\odot)$	0.432(109)	0.500(124)	1.293(315)	3.582(748)
$M_{\rm bol}$(mag.)	5.641(243)	5.483(241)	4.451(237)	3.345(206)
$\log(g)(cgs)$	4.449(23)	4.473(32)	4.213(10)	4.288(27)
$a(R_\odot)$	2.063(195)		2.669(224)	

$M_{\rm bol\odot} = 4.73^{\rm mag}$.

$$M_{\rm bol(\mathit{h},\mathit{c})} = M_{\rm bol\odot} - 2.5 \times \log\left(\frac{L_{(\mathit{h},\mathit{c})}}{L_\odot}\right). \quad (9)$$

Table 3 lists the values of the estimated absolute parameters. The uncertainties of each absolute parameter in this study are computed using the a–P relationship results and the light curve solution parameters ($r_{\rm mean(\mathit{h},\mathit{c})}$, $T_{(\mathit{h},\mathit{c})}$, and q).

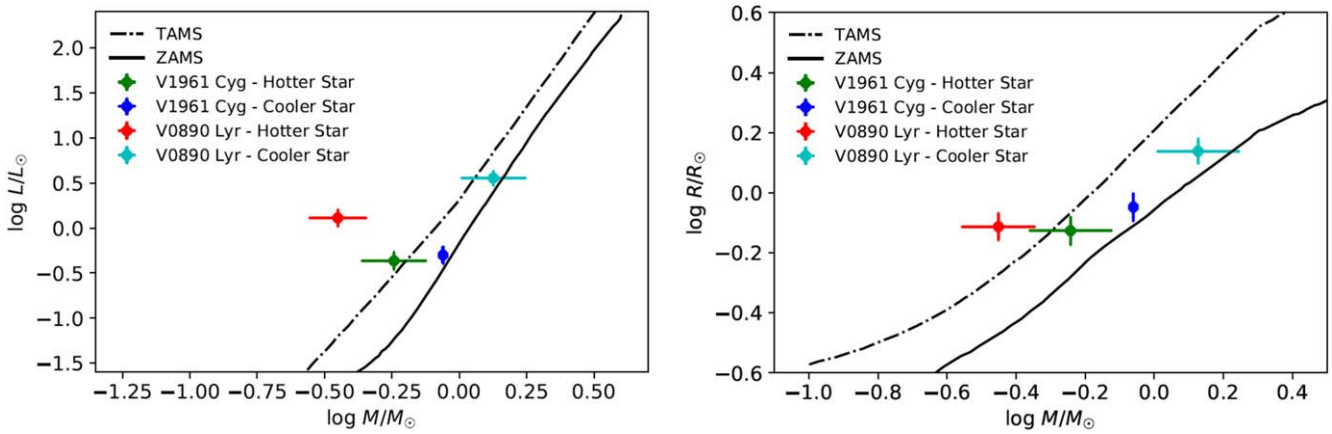

Figure 9. Both systems are displayed in a Mass–Luminosity diagram (left) and a Mass–Radius diagram (right) along with the ZAMS and TAMS limits.

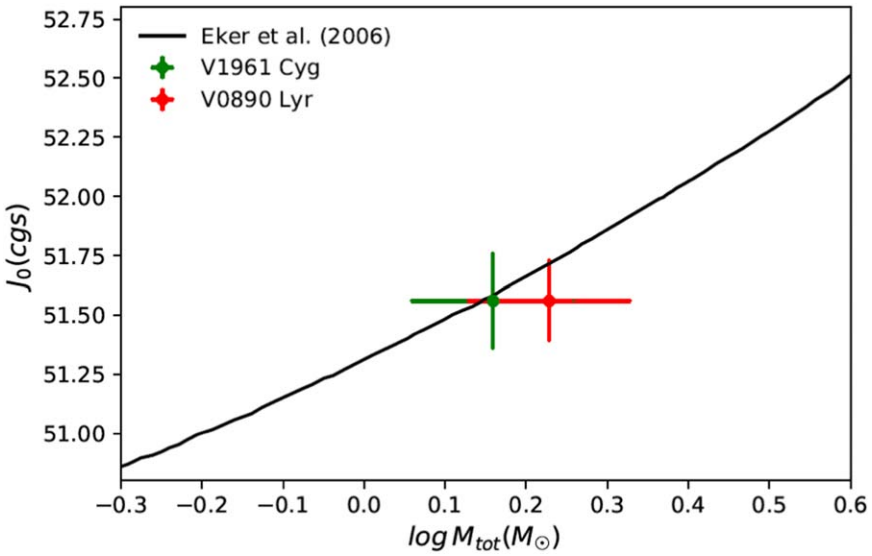

Figure 10. Diagram of orbital angular momentum of each system as a function of total mass.

Table 4
Some of the q–L_{ratio} Relationships Presented by Previous Investigations for Contact Binary Systems

Relationship	References
$L_2/L_1 = (M_2/M_1)^{0.92}$	Lucy (1968a)
$L_2/L_1 = (M_2/M_1)^{0.96}$	Lucy (1968b)
$L_2/L_1 = (M_2/M_1)^{0.92}$	Copeland et al. (1970)
$L_2/L_1 = (M_2/M_1)^{0.93}$	Habets & Heintze (1981)
$L_2/L_1 = (M_2/M_1)^{0.82}$	Rovithis-Livaniou et al. (1992)
$L_2/L_1 = (M_2/M_1)^{1.04}$	Rovithis-Livaniou et al. (1992)
$L_2/L_1 = (M_2/M_1)^{0.74}$	Awadalal & Hanan (2005)
$L_2/L_1 = (M_2/M_1)^{0.72}$	Poro et al. (2024c)

6. Discussion and Conclusion

We employed ground-based photometric observations to investigate two W UMa-type contact binary systems. V1961 Cyg and V0890 Lyr were observed during five nights in 2023 at an observatory in France. We extracted four primary and secondary times of minima from our data for both target systems and presented new ephemerides.

The first light curve analysis of the systems was done using PHOEBE and MCMC. We used the q-search method on photometric data to determine the initial mass ratio. The final parameter and uncertainty results were obtained after

Table 5
The Sample Used for the Relationship between the Mass Ratio and the Luminosity Ratio

System	$1/q$	L_{ratio}	References	System	$1/q$	L_{ratio}	References
AA UMa	0.551	1.177	Lee et al. (2011)	NN Vir	0.491	1.021	Deb & Singh (2011)
AB And	0.560	1.687	Li et al. (2014)	NSVS 4161544	0.296	0.842	Kjurkchieva et al. (2019)
AD Phe	0.376	0.990	Pi et al. (2017)	NSVS 13392702	0.510	1.961	Lohr et al. (2014)
AH Aur	0.165	0.334	Gazeas et al. (2005)	OO Aql	0.846	1.669	Li et al. (2016a)
AP Leo	0.297	0.690	Kreiner et al. (2003)	OU Ser	0.173	0.583	Deb & Singh (2011)
AQ Tuc	0.354	0.595	Chochol et al. (2001)	QX And	0.306	0.742	Djurašević et al. (2011)
AU Ser	0.692	1.790	Alton et al. (2018b)	RT LMi	0.382	1.019	Zola et al. (2010)
BB Peg	0.318	0.880	Kamalifar et al. (2020)	RW Com	0.471	1.984	Deb & Singh (2011)
BI CVn	0.413	1.075	Nelson et al. (2014)	RW Dor	0.630	2.207	Sarotsakulchai et al. (2019)
BN Ari	0.392	1.309	Alton et al. (2018a)	RZ Tau	0.376	0.905	Yang & Liu (2003)
BO Ari	0.190	0.597	Gürol et al. (2015c)	SW Lac	0.787	2.454	Gazeas et al. (2005)
BX Dra	0.288	0.497	Park et al. (2013)	SX Crv	0.079	0.250	Zola et al. (2004)
BX Peg	0.376	1.341	Li et al. (2015a)	TV Mus	0.166	0.372	Qian et al. (2005)
CC Com	0.526	2.383	Köse et al. (2011)	TW Cet	0.750	2.367	Deb & Singh (2011)
CK Boo	0.111	0.313	Deb & Singh (2011)	TX Cnc	0.455	1.188	Deb & Singh (2011)
CN And	0.387	0.836	Yildirim et al. (2019)	TY Pup	0.250	0.305	Sarotsakulchai et al. (2018)
DK Cyg	0.307	0.652	Lee et al. (2015)	TY UMa	0.396	1.117	Li et al. (2015b)
DN Boo	0.103	0.230	Şenavcı et al. (2008)	U Peg	0.331	0.883	Djurašević et al. (2001)
DN Cam	0.442	0.887	Baran et al. (2004)	UV Lyn	0.372	0.896	Zola et al. (2005)
DX Tuc	0.290	0.769	Szalai et al. (2007)	UX Eri	0.373	0.838	Deb & Singh (2011)
DY Cet	0.356	0.808	Deb & Singh (2011)	V1073 Cyg	0.303	0.386	Tian et al. (2018)
DZ Psc	0.136	0.371	Yang et al. (2013)	V1128 Tau	0.534	1.749	Çalışkan et al. (2014)
EF Boo	0.531	1.773	Paki & Poro (2024)	V1191 Cyg	0.107	0.341	Ostadnezhad et al. (2014)
EQ Tau	0.439	1.286	Hasanzadeh et al. (2015)	V1453 Her	0.670	2.958	Lohr et al. (2014)
ET Leo	0.342	0.987	Gazeas et al. (2006)	V1918 Cyg	0.278	0.673	Gürol (2016)
EX Leo	0.200	0.489	Zola et al. (2010)	V2357 Oph	0.231	0.556	Deb & Singh (2011)
EZ Hya	0.257	0.571	Yang et al. (2004)	V2377 Oph	0.395	0.929	Deb & Singh (2011)
FG Hya	0.104	0.317	Zola et al. (2010)	V351 Peg	0.360	0.607	Albayrak et al. (2005)
FP Boo	0.096	0.150	Gazeas et al. (2006)	V357 Peg	0.401	0.693	Ekmekçi et al. (2012)
FU Dra	0.251	0.818	Liu et al. (2012)	V402 Aur	0.200	0.331	Zola et al. (2004)
GM Dra	0.210	0.620	Gazeas et al. (2005)	V404 Peg	0.243	0.580	Gürol et al. (2011)
GR Vir	0.106	0.306	Gazeas et al. (2005)	V417 Aql	0.362	0.978	Deb & Singh (2011)
GSC 03 334-00553	0.421	1.118	Kjurkchieva et al. (2019)	V535 Ara	0.302	0.480	Özkardeş & Erdem (2012)
GW Cnc	0.265	0.942	Gürol et al. (2016)	V546 And	0.254	0.663	Gürol et al. (2015b)
HH Boo	0.587	1.842	Gürol et al. (2015a)	V781 Tau	0.453	1.313	Li et al. (2016b)
HI Pup	0.206	0.476	Ulaş & Ulusoy (2014)	V829 Her	0.435	1.215	Erdem & Özkardeş (2006)
HN UMa	0.145	0.379	Oh et al. (2007)	V839 Oph	0.305	0.746	Deb & Singh (2011)
HV Aqr	0.145	0.387	Li & Qian (2013)	V870 Ara	0.082	0.205	Szalai et al. (2007)
HV UMa	0.190	0.535	Csák et al. (2000)	V972 Her	0.164	0.370	Selam et al. (2018)
KIC 10 618 253	0.125	0.286	Şenavcıet al. (2016)	VW Boo	0.428	1.250	Liu et al. (2011)
KIC 9 832 227	0.228	0.498	Molnar et al. (2017)	VW Cep	0.302	1.085	Mitnyan et al. (2018)
LO And	0.305	0.802	Nelson & Robb (2015)	VY Sex	0.313	0.706	Deb & Singh (2011)
LS Del	0.375	1.031	Deb & Singh (2011)	XX Sex	0.100	0.185	Deb & Singh (2011)
MW Pav	0.220	0.277	Alvarez et al. (2015)	YY CrB	0.232	0.616	Gazeas et al. (2005)

performing the MCMC process. Therefore, the companion temperature difference is 287 K and 238 K for V1961 Cyg and V0890 Lyr, respectively. The spectral types of stars in V1961 Cyg and stars in V0890 Lyr were determined to be G8-K1 and F1-F2, respectively, based on the Eker et al. (2018) and Cox (2015) studies.

We used a new method to examine the mass ratios resulting from our light curve solutions. Kouzuma (2023) presented a method for estimating the photometric mass ratio of overcontact binaries using derivatives of the light curve. Most overcontact systems can employ this new method. The basis of this method is derivation at various orders of the photometric light curve. The light curve should show at least two maxima after the derivative. A parameter named W is obtained after the third-order derivative. According to Kouzuma (2023), there is a strong relationship between W and q. We used this method for V1961 Cyg and V0890 Lyr, and the results were mass ratios of $1/q = 0.681(72)$ and $1/q = 0.268(43)$, respectively. We found close mass ratio estimates with a discrepancy of $\Delta q = 0.023$ and $\Delta q = 0.003$ for V1961 Cyg and V0890 Lyr, respectively,

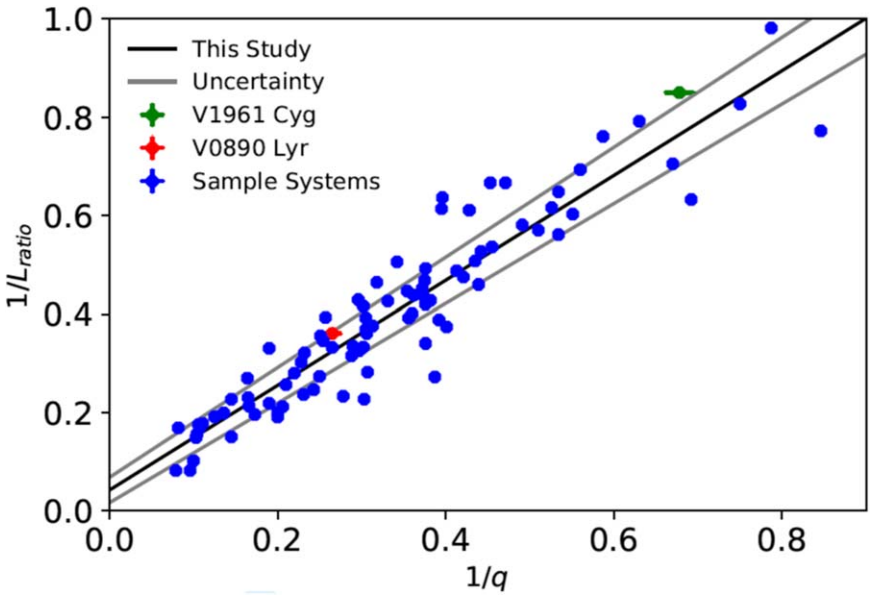

Figure 11. q–$L_{\rm ratio}$ diagram using 88 contact binary systems and a linear fit on the points.

between our light curve analysis results and the Kouzuma (2023) study. Figure 8 shows the derivative process of the light curves.

The estimation of the absolute parameters was presented using the relationship between the semimajor axis and the orbital period. Based on the estimated absolute parameters, we displayed the state of evolution of the target systems on the Mass–Luminosity (M–L) and Mass–Radius (M–R) diagrams. The theoretical Zero-Age Main Sequence (ZAMS) and Terminal-Age Main Sequence (TAMS) lines are also displayed based on the study of Girardi et al. (2000) on the $M-L$ and $M-R$ diagrams (Figure 9). In the $M-L$ and $M-R$ diagrams, the hotter star of V1961 Cyg is near the TAMS line, whereas for V0890 Lyr, it is above the TAMS. The cooler star is located between ZAMS and TAMS for both target systems.

The orbital angular momentum (J_0) was computed for V1961 Cyg and V0890 Lyr to be $J_0 = 51.56 \pm 0.20$ and $J_0 = 51.56 \pm 0.17$, respectively, based on the orbital period, mass ratio, and total mass of the systems. We estimated J_0 using Equation (10) that the Eker et al. (2006) study provided.

$$J_0 = \frac{q}{(1+q)^2}\sqrt[3]{\frac{G^2}{2\pi}M^5P}. \quad (10)$$

Furthermore, the $\log M_{\rm tot}$–$\log J_0$ diagram (Figure 10) shows the system's position and indicates that both systems are located in the region of contact binary systems.

In the literature, there are studies about the empirical relationship between the mass ratio (q) and the luminosity ratio ($L_{\rm ratio}$) for contact binary systems. We have listed some of the relationships presented in these studies in Table 4. We updated the q–$L_{\rm ratio}$ relationship based on a valid sample.

We chose a sample for the q–$L_{\rm ratio}$ relationship from the Latković et al. (2021) study. Therefore, we only selected studies that had or used spectroscopic results. We excluded from the sample the results that contained l_3, or if l_3 in subsequent studies was present for that system. Also, we are not considering the studies that used low-resolution spectroscopic observations. The systems used for this sample include both subtypes A and W. As a result, we have listed the remaining 88 contact binary systems for the sample in Table 5. We used a linear fit on the points, whose equation is as follows.

$$q = (1.066 \pm 0.052)L_{\rm ratio} + (0.042 \pm 0.019). \quad (11)$$

The mass ratio and luminosity ratio in Equation (11) are expressed as $1/q$ and $1/L_{\rm ratio}$, respectively, and have not been utilized in previous studies of similar form (Table 4). It seems that in this form, there is less scattering in the data points than in other samples. Additionally, mass ratios from both kinds of photometric and spectroscopic data can be found in other literature samples. The position of the V1961 Cyg and V0890 Lyr systems in Figure 11 is in agreement with other contact systems that have spectroscopic data analyzed.

We used the $i > \arccos|(r_1 - r_2)/a|$ relationship from the Sun et al. (2020) study to find that the target systems are partially or totally eclipsing systems. Therefore, V1961 Cyg with $i = 88.^{\circ}57$ is total, and V0890 Lyr with $i = 67.^{\circ}00$ is a partial binary system. Based on the discussion of the Terrell & Wilson (2005) study, systems with total and partial eclipses with high orbital inclinations can have acceptable photometric

mass ratios. Also, according to the mass ratio from the light curve solutions in the MCMC process, the mass ratio results using the Kouzuma (2023) method, and their position in the empirical relationship of q–$L_{\rm ratio}$, the obtained mass ratios are relabeled for both systems.

According to the mass ratios, fillout factors, and orbital inclinations of the target systems, we can conclude that V1961 Cyg and V0890 Lyr are contact binary systems. Based on the fillout factor, there are three categories: deep ($f \geqslant 50\%$), medium ($25\% \leqslant f < 50\%$), and shallow ($f < 25\%$) eclipsing contact binary stars (Li et al. 2022). So, V1961 Cyg is shallow, and V0890 Lyr is a medium system. Additionally, contact binaries are divided into A- and W-subtypes (Binnendijk 1970). The more massive component is a hotter star in the A-subtype, and if the less massive component has a higher effective temperature, it is classified as a W-subtype. Therefore, based on the results of the light curve solutions and the estimation of absolute parameters, they are categorized as a W-subtype since the less massive component has higher effective temperatures.

Acknowledgments

This manuscript was prepared by the BSN (https://bsnp.info/) project. We have made use of data from the European Space Agency (ESA) mission Gaia (http://www.cosmos.esa.int/gaia), processed by the Gaia Data Processing and Analysis Consortium (DPAC).

Data Availability

Ground-based data will be made available on request.

ORCID iDs

Sabrina Baudart https://orcid.org/0009-0004-8426-4114
Atila Poro https://orcid.org/0000-0002-0196-9732

References

Albayrak, B., Djurašević, G., Selam, S. O., Atanacković-Vukmanović, O., & Yılmaz, M. 2005, NewA, 10, 163
Alton, K. B., Nelson, R. H., & Boyd, D. R. S. 2018a, AcA, 68, 159
Alton, K. B., Nelson, R. H., & Terrell, D. 2018b, IBVS, 6256, 1
Alvarez, G. E., Sowell, J. R., Williamon, R. M., & Lapasset, E. 2015, PASP, 127, 742
Awadalla, N. S., & Hanna, M. A. 2005, JKAS, 38, 43
Baran, A., Zola, S., Rucinski, S. M., et al. 2004, AcA, 54, 195
Binnendijk, L. 1970, VA, 12, 217
Çalışkan, Ş., Latković, O., Djurašević, G., et al. 2014, AJ, 148, 126
Castelli, F., & Kurucz, R. 2004, A&A, 419, 725
Chochol, D., van Houten, C. J., Pribulla, T., & Grygar, J. 2001, CoSka, 31, 5
Conroy, K. E., Kochoska, A., Hey, D., et al. 2020, ApJS, 250, 34
Copeland, H., Jensen, J. O., & Jorgensen, H. E. 1970, A&A, 5, 12
Cox, A. N. 2015, Allen's astrophysical quantities (Berlin: Springer)
Csák, B., Kiss, L. L., Vinkó, J., & Alfaro, E. J. 2000, A&A, 356, 603
Deb, S., & Singh, H. P. 2011, MNRAS, 412, 1787
Djurašević, G., Rovithis-Livaniou, H., Rovithis, P., Erkapić, S., & Milovanović, N. 2001, A&A, 367, 840
Djurašević, G., Yılmaz, M., Baştürk, Ö., et al. 2011, A&A, 525, A66
Eker, Z., Bakış, V., Bilir, S., et al. 2018, MNRAS, 479, 5491
Eker, Z., Demircan, O., Bilir, S., & Karataş, Y. 2006, MNRAS, 373, 1483
Ekmekçi, F., Elmaslı, A., Yılmaz, M., et al. 2012, NewA, 17, 603
Erdem, A., & Özkardeş, B. 2006, NewA, 12, 192
Foreman-Mackey, D., Hogg, D. W., Lang, D., & Goodman, J. 2013, PASP, 125, 306
Gazeas, K. D., Baran, A., Niarchos, P., et al. 2005, AcA, 55, 123
Gazeas, K. D., Niarchos, P. G., Zola, S., Kreiner, J. M., & Rucinski, S. M. 2006, AcA, 56, 127
Gettel, S. J., Geske, M. T., & McKay, T. A. 2006, AJ, 131, 621
Girardi, L., Bressan, A., Bertelli, G., & Chiosi, C. 2000, A&AS, 141, 371
Guo, D.-F., Li, K., Liu, F., et al. 2022, MNRAS, 517, 1928
Gürol, B. 2016, NewA, 47, 57
Gürol, B., Bradstreet, D. H., Demircan, Y., & Gürsoytrak, S. H. 2015a, NewA, 41, 26
Gürol, B., Bradstreet, D. H., & Okan, A. 2015b, NewA, 36, 100
Gürol, B., Gökay, G., Saral, G., et al. 2016, NewA, 46, 31
Gürol, B., Gürsoytrak, S. H., & Bradstreet, D. H. 2015c, NewA, 39, 9
Gürol, B., Terzioğlu, Z., Gürsoytrak, S. H., Gökay, G., & Derman, E. 2011, AN, 332, 690
Habets, G. M. H. J., & Heintze, J. R. W. 1981, A&AS, 46, 193
Hasanzadeh, A., Farsian, F., & Nemati, M. 2015, NewA, 34, 262
Hogg, D. W., & Foreman-Mackey, D. 2018, ApJS, 236, 11
Hubscher, J., Paschke, A., & Walter, F. 2005, IBVS, 5657, 1
Kamalifar, Z., Abedi, A., & Roobiat, K. Y. 2020, NewA, 78, 101354
Kjurkchieva, D., Stateva, I., Popov, V. A., & Marchev, D. 2019, AJ, 157, 73
Kopal, Z. 1959, Close Binary Systems (London: Chapman & Hall)
Köse, O., Kalomeni, B., Keskin, V., Ulaş, B., & Yakut, K. 2011, AN, 332, 626
Kouzuma, S. 2023, ApJ, 958, 84
Kreiner, J. M., Rucinski, S. M., Zola, S., et al. 2003, A&A, 412, 465
Kuiper, G. P. 1941, ApJ, vol. 93, 133
Kulagin, Y. V., & Shugarov, S. Y. 1989, ATsir, 1541, 11
Latković, O., Čeki, A., & Lazarević, S. 2021, ApJS, 254, 10
Lee, J. W., Lee, C.-U., Kim, S.-L., Kim, H.-I., & Park, J.-H. 2011, PASP, 123, 34
Lee, J. W., Youn, J.-H., Park, J.-H., & Wolf, M. 2015, AJ, 149, 194
Li, H.-L., Wei, J.-Y., Yang, Y.-G., & Dai, H.-F. 2016a, RAA, 16, 2
Li, K., Gao, D. Y., Hu, S. M., et al. 2016b, Ap&SS, 361, 63
Li, K., Gao, X., Liu, X.-Y., et al. 2022, AJ, 164, 202
Li, K., Hu, S., Guo, D., et al. 2015a, NewA, 41, 17
Li, K., Hu, S. M., Guo, D. F., et al. 2015b, AJ, 149, 120
Li, K., Hu, S. M., Jiang, Y. G., Chen, X., & Ren, D. Y. 2014, NewA, 30, 64
Li, K., & Qian, S. B. 2013, NewA, 21, 46
Liu, L., Qian, S.-B., He, J.-J., et al. 2012, PASJ, 64, 48
Liu, L., Qian, S. B., Zhu, L. Y., He, J. J., & Li, L. J. 2011, AJ, 141, 147
Lohr, M. E., Hodgkin, S. T., Norton, A. J., & Kolb, U. C. 2014, A&A, 563, A34
Loukaidou, G. A., Gazeas, K. D., Palafouta, S., et al. 2022, MNRAS, 514, 5528
Lucy, L. B. 1967, ZA, 65, 89
Lucy, L. B. 1968a, ApJ, 153, 877
Lucy, L. B. 1968b, ApJ, 151, 1123
Lucy, L. B., & Wilson, R. E. 1979, ApJ, 231, 502
Mitnyan, T., Bódi, A., Szalai, T., et al. 2018, A&A, 612, A91
Molnar, L. A., Van Noord, D. M., Kinemuchi, K., et al. 2017, ApJ, 840, 1
Nelson, R. H., Şenavci, H. V., Baştürk, Ö., & Bahar, E. 2014, NewA, 29, 57
Nelson, R. H., & Robb, R. M. 2015, IBVS, 6134, 1
O'Connell, D. 1951, MNRAS, 111, 642
Oh, K. D., Kim, C. H., Kim, H. I., & Lee, W. B. 2007, in ASP Conf, Ser. 362, The Seventh Pacific Rim Conference on Stellar Astrophysics, ed. Y. W. Kang et al. (San Francisco, CA: ASP), 82
Ostadnezhad, S., Delband, M., & Hasanzadeh, A. 2014, NewA, 31, 14
Özkardeş, B., & Erdem, A. 2012, NewA, 17, 143
Pagel, L. 2022, AIAAJ, 60, 1
Paki, E., & Poro, A. 2024, Ap, 67, 316
Park, J.-H., Lee, J. W., Kim, S.-L., Lee, C.-U., & Jeon, Y.-B. 2013, PASJ, 65, 1
Pi, Q.-f., Zhang, L.-y., Bi, S.-l., et al. 2017, AJ, 154, 260
Pogson, N. 1856, MNRAS, 17, 12
Poro, A., Hedayatjoo, M., Nastaran, M., et al. 2024b, NewA, 110, 102227
Poro, A., Paki, E., Alizadehsabegh, A., et al. 2024c, RAA, 24, 015002

Poro, A., Tanriver, M., Michel, R., & Paki, E. 2024a, PASP, 136, 024201
Prša, A., Conroy, K. E., Horvat, M., et al. 2016, ApJS, 227, 29
Qian, S. B., Yang, Y. G., Soonthornthum, B., et al. 2005, AJ, 130, 224
Rovithis-Livaniou, H., Rovithis, P., & Bitzaraki, O. 1992, Ap&SS, 189, 237
Rucinski, S. 1969, AcA, 19, 245
Sarotsakulchai, T., Qian, S. B., Soonthornthum, B., et al. 2018, AJ, 156, 199
Sarotsakulchai, T., Qian, S.-B., Soonthornthum, B., et al. 2019, PASJ, 71, 34
Selam, S. O., Esmer, E. M., Şenavcı, H. V., et al. 2018, Ap&SS, 363, 34
Şenavcı, H. V., Doğruel, M. B., Nelson, R. H., Yılmaz, M., & Selam, S. O. 2016, PASA, 33, e043
Şenavcı, H. V., Nelson, R. H., Özavcı, İ, Selam, S. O., & Albayrak, B. 2008, NewA, 13, 468
Sun, W., Chen, X., Deng, L., & de Grijs, R. 2020, ApJS, 247, 50
Szalai, T., Kiss, L. L., Mészáros, S., Vinkó, J., & Csizmadia, S. 2007, A&A, 465, 943
Terrell, D., & Wilson, R. E. 2005, Ap&SS, 296, 221
Tian, X.-M., Zhu, L.-Y., Qian, S.-B., Li, L.-J., & Jiang, L.-Q. 2018, RAA, 18, 020
Torres, G. 2010, AJ, 140, 1158
Ulaş, B., & Ulusoy, C. 2014, NewA, 31, 56
Yakut, K., & Eggleton, P. P. 2005, ApJ, 629, 1055
Yang, Y., & Liu, Q. 2003, AJ, 126, 1960
Yang, Y. G., Qian, S. B., Zhang, L. Y., Dai, H. F., & Soonthornthum, B. 2013, AJ, 146, 35
Yang, Y. G., Qian, S. B., & Zhu, C. H. 2004, PASP, 116, 826
Yildirim, M. F., Aliçavuş, F., & Soydugan, F. 2019, RAA, 19, 010
Zhang, X.-D., & Qian, S.-B. 2020, MNRAS, 497, 3493
Zola, S., Gazeas, K., Kreiner, J. M., et al. 2010, MNRAS, 408, 464
Zola, S., Kreiner, J. M., Zakrzewski, B., et al. 2005, AcA, 55, 389
Zola, S., Rucinski, S. M., Baran, A., et al. 2004, AcA, 54, 299